Developmental Cell *19*

Supplemental Information

Integrin-Linked Kinase Controls Microtubule Dynamics Required for Plasma Membrane Targeting of Caveolae

Sara A. Wickström, Anika Lange, Michael W. Hess, Julien Polleux, Joachim P. Spatz, Marcus Krüger, Kristian Pfaller, Armin Lambacher, Wilhelm Bloch, Matthias Mann, Lukas A. Huber, and Reinhard Fässler

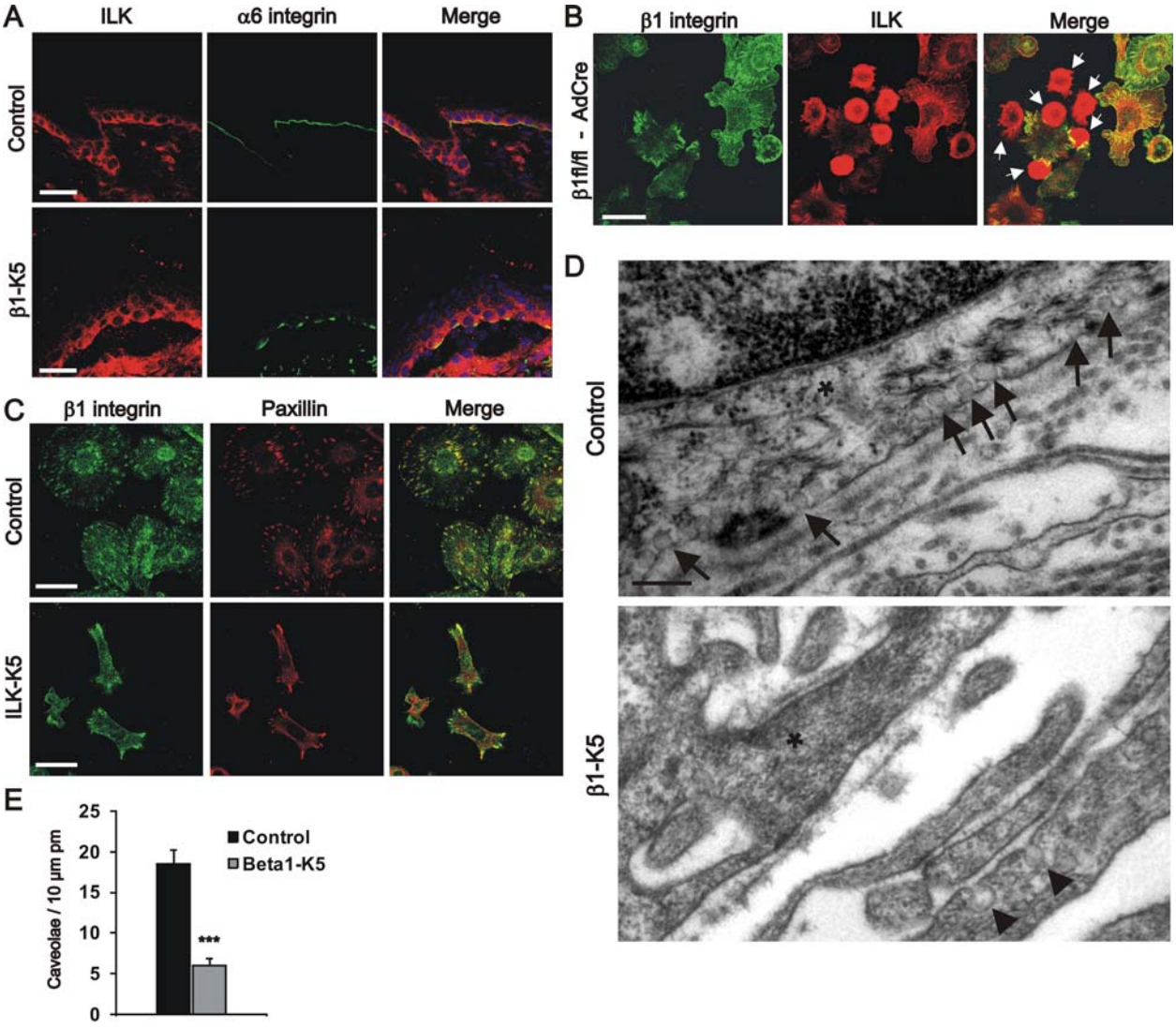

Figure S1. β1 integrin regulates ILK and caveolae (related to Fig. 1)
(A) Control and β1-K5 skin stained for ILK and α6 integrin. Loss of basal targeting of ILK is observed in β1-K5 keratinocytes. Scale bar 25 µm. **(B)** β1 fl/fl keratinocytes were adenovirally transduced with *Cre*

recombinase (AdCre) to delete β1 integrin, after which the mixed cell population was stained for β1 integrin and ILK. ILK is localized diffusely in the cytoplasm of cells lacking β1 (arrowheads). Scale bar 30 μm. **(C)** ILK-K5 keratinocytes stained for β1 integrin and paxillin. Scale bar 30 μm. **(D)** EM of control and β1-K5 skin. Decreased amounts of plasma membrane caveolae (arrows) are seen in the basal keratinocytes (asterisk) in the absence of β1. Note multiple caveolae in dermal cells of β1-K5 mice, where β1 integrin is not deleted (arrowheads). Scale bar 200 nm. **(E)** Quantification of plasma membrane caveolae from control and β1-K5 skin (mean±SEM, n=3/3, ***p<0.0001). β1-K5 mice show decreased levels of plasma membrane (pm) caveolae in the skin.

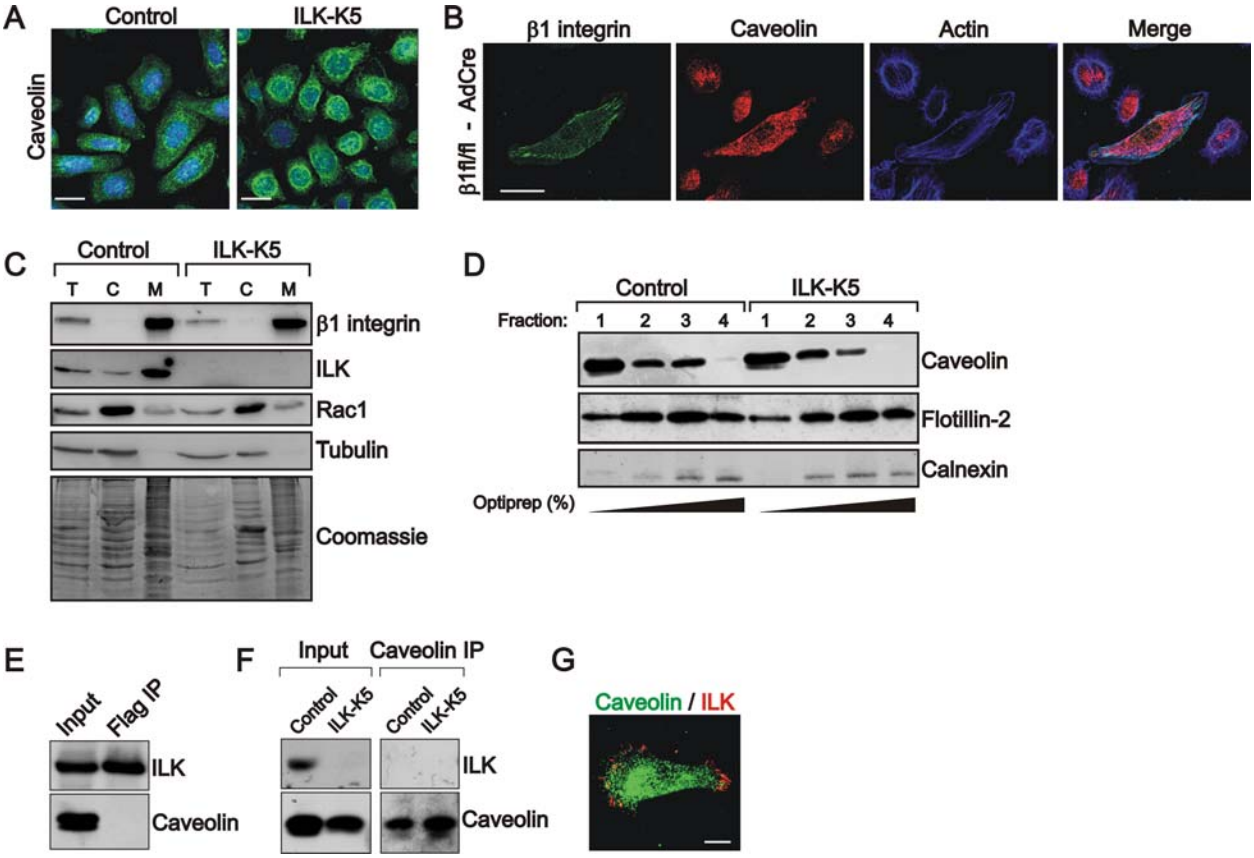

Figure S2. ILK regulates caveolae formation (related to Fig. 1 and 2)
(A) Keratinocytes stained for caveolin-1. Note increased perinuclear localization of caveolin-1 in ILK-K5 cells. Scale bars 20 μm. (**B)** β1fl/fl keratinocytes infected with adenoviral *Cre* (Ad-Cre) and stained for β1 integrin, caveolin, and F-actin. Note perinuclear localization of caveolin in cells lacking β1 expression. Scale bar 20 μm. **(C)** Levels of Rac1 in membrane fractions were analyzed by Western blotting. β1 integrin serves as a loading control for the membrane fraction (M), and tubulin for the total (T) and cytosolic (C) fractions. **(D)** DRMs isolated from keratinocytes using an Optiprep density gradient. Caveolin-1 is detected in the light fractions of the gradient. Flotillin-2, a known raft protein, and calnexin, a membrane protein not found in rafts, were used as controls. **(E)** Caveolin-1 is not detected in ILK immunoprecipitates. **(F)** ILK is not detected in caveolin-1 immunoprecipitates. **(G)** ILK and caveolin-1 do not co-localize in keratinocytes. Scale bar 10 μm.

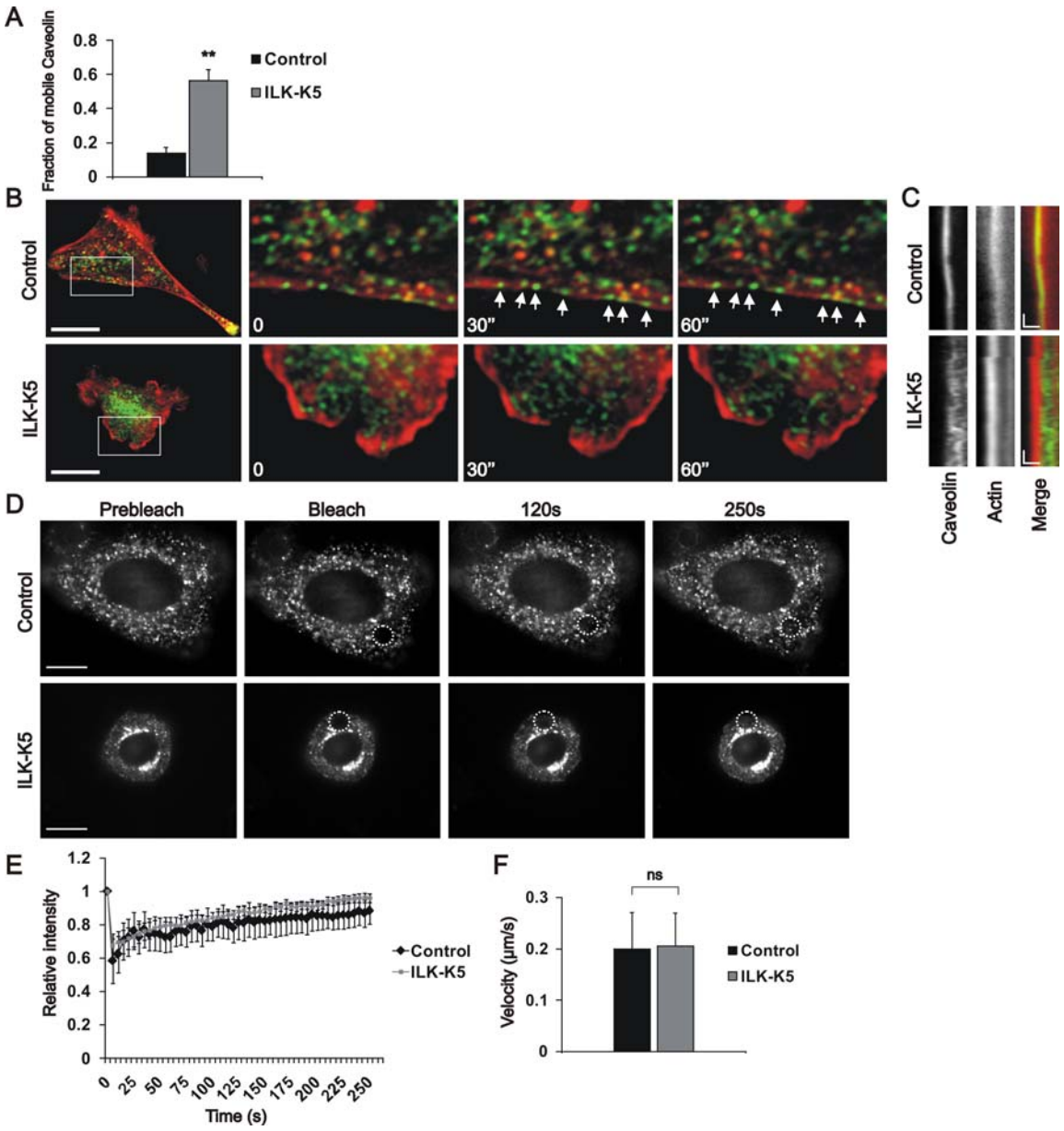

Figure S3. Altered motility of caveolae in ILK-K5 cells (related to Fig. 3)
(A) Quantification of of motile caveolae in cells adhering on 20 µm-sized micropatterns and visualized by TIRF microscopy. (mean±SEM, n=6/6, **p=0.0079) **(B)** Dynamics of caveolae (green) and actin (red) analyzed by spinning disc microscopy in control and ILK-K5 keratinocytes. Images shown are snapshots from movies acquired 1 s/frame. Right panels show an enlargement of the area indicated by a white rectangle. Arrowheads indicate vesicles co-localizing with cortical actin. Scale bars 10 µm. **(C)** Kymographs from cells in panel (a) show motile caveolae but a stable lamella in ILK-K5 cells. Scale bars 30 s (y axis); 2 µm (x axis). **(D)** EGFP-Caveolin-1 expressing keratinocytes were subjected to photobleaching after which recovery was followed by time lapse microscopy. Images shown are snapshots from movies acquired before bleaching and during recovery. The bleached area is marked by a dotted circle. Scale bars 5 µm. **(E)** Quanitification of recovery after photobleaching Note similar rates of recovery in control and ILK-K5 cells (mean±SEM, n=7/7). **(F)** Velocities of individual intracellular caveolae measured by manual tracking. Caveolae in control and ILK-K5 cells move with comparable velocity (mean±SEM, n=12/12). ns=not significant.

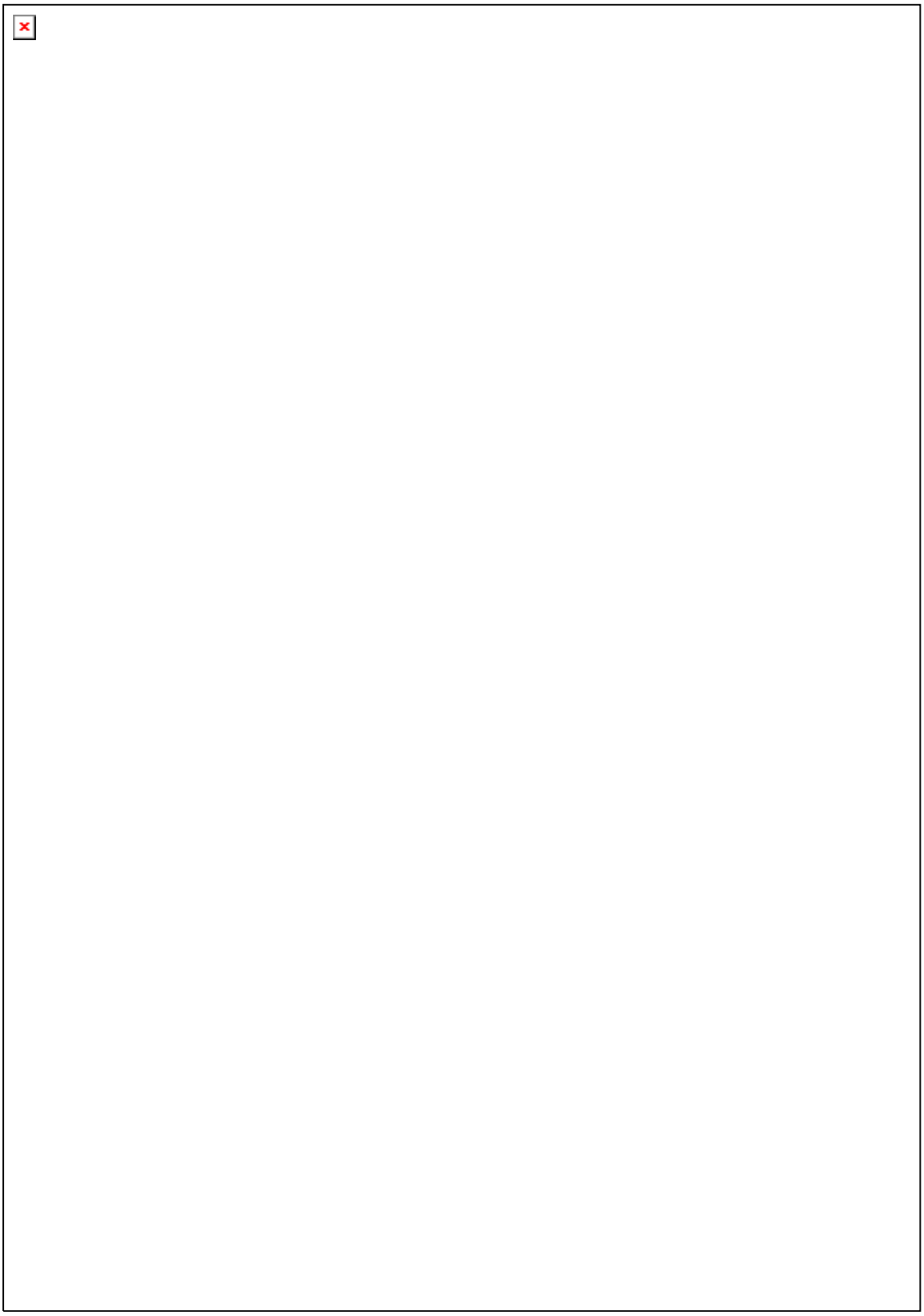

Figure S4. IQGAP1 and mDia1 regulate caveolin localization (related to Fig. 6-8)
(A) Control and ILK-K5 cells plated on 20 μm-sized micropatterns and for IQGAP1 and actin. Note cortical localization of IQGAP1 in control cells. Scale bars 10 μm. **(B)** Control and IQGAP1 or mDia1 siRNA transfected cells stained for β1 integrin and paxillin. **(C)** Control and IQGAP1 or mDia1 siRNA transfected cells analyzed for β1 integrin cell surface expression levels using flow cytometry (mean

±SEM, n=3/3/3). **(D)** Control and ILK-K5 cells stained for mDia1 and actin. Note cortical localization of mDia1 in control cells. **(E)** mDia1 protein levels analyzed by Western blotting. mDia levels are reduced in ILK-K5 cells but can be restored by re-expressing EGFP-ILK. **(F)** Western blot analysis of cells transfected with control or IQGAP1 siRNA together with EGFP-IQGAP1 or deletion mutants. **(G)** Cells were transfected with control or IQGAP1 siRNA together with EGFP-IQGAP1, deletion mutants or vector and stained with antibodies against acetylated tubulin. Decreased levels of acetylated tubulin is seen in IQGAP1-depleted cells. This is rescued with full length IQGAP1 but not mutants. Scale bars 20 µm. **(H)** Control and mDia1 siRNA transfected cells stained with antibodies against caveolin-1 and actin. Note increased perinuclear localization of caveolin-1 in mDia1-depleted cells.

Table S1. Parameters of MT dynamic instability

(A) Parameters of MT dynamic instability in control and ILK-K5 cells.

	Control	ILK-K5
Growth rate (µm/min)	8.23±0.45	7.24±0.94
Shortening rate (µm/min)	12.85±1.30	11.37±1.3
Catastrophe frequency (s^{-1})	0.010±0.002	0.030±0.003***
Rescue frequency (s^{-1})	0.011±0.002	0.023±0.003**
Duration of pauses (s)	48.2±8.8	20.6±1.2**
Number of analyzed MTs	47	49
Number of analyzed cells	7	9

Values are mean ±SEM; ***p=0.0006, **p=0.0059 (rescue frequency) and 0.0013 (duration of pauses).

(B) Parameters of MT dynamic instability in control keratinocytes transfected with scrambled, IQGAP1, or mDia1 siRNA.

	Scrambled control	IQGAP1 siRNA	mDia1 siRNA
Growth rate (µm/min)	9.23±0.53	10.91±0.59	10.36±0.74
Shortening rate (µm/min)	11.89±0.60	12.67±1.45	13.71±1.06
Catastrophe frequency (s^{-1})	0.019±0.002	0.031±0.002**	0.032±0.003**
Rescue frequency (s^{-1})	0.016±0.0009	0.026±0.001**	0.030±0.002**
Duration of pauses (s)	34.8±2.7	21.19±1.88**	19.23±3.215**
Number of analyzed MTs	41	36	30
Number of analyzed cells	7	3	5

Values are mean ±SEM; **p=0.0012 (catastrophe and rescue frequency; IQGAP1 siRNA), 0.0025 (rescue frequency; mDia siRNA), 0.010 (catastrophe frequency; mDia siRNA), 0.0047 (duration of pauses; IQGAP1 siRNA), and 0.0051 (duration of pauses; mDia siRNA).

(C) Parameters of MT dynamic instability in ILK-K5 cells and ILK-K5 cells expressing active mDia FH1FH2.

	ILK-K5	ILK-K5 mDiaFH1FH2
Growth rate (µm/min)	7.24±0.94	7.92±0.55
Shortening rate (µm/min)	11.37±1.3	12.06±1.16
Catastrophe frequency (s^{-1})	0.030±0.003	0.018±0.001**
Rescue frequency (s^{-1})	0.023±0.003	0.011±0.001**
Duration of pauses (s)	20.6±1.2	35.9±3.3***
Number of analyzed MTs	49	47
Number of analyzed cells	9	8

Values are mean ±SEM; ***p=0.0002, **p=0.0019 (catastrophe frequency) and 0.0011 (rescue frequency).

Supplemental Experimental Procedures

Antibodies

Rabbit anti-caveolin-1, mouse anti-ILK, mouse anti-mDia1, mouse anti-IQGAP1, mouse anti-calnexin, mouse anti-flotillin-2, mouse anti-EEA1, mouse anti-paxillin, mouse anti-Rac1, and FITC-conjugated integrin α6 antibodies were from BD Biosciences. Mouse anti-transferrin receptor (Tfr) was from Zymed, rabbit anti-IQGAP1 was from Santa Cruz Biotech, rat anti-α-tubulin and rat anti-β1 integrin from Chemicon, rabbit anti-α-tubulin and rabbit anti-FLAG from Cell Signaling, mouse anti-acetylated tubulin and rabbit anti-actin were from Sigma, and mouse anti-GAPDH was from Calbiochem. Secondary antibodies used for immunofluorescence were from Invitrogen (Alexa488, Alexa647) and Jackson ImmunoResearch Laboratories (Cy3).

Electron microscopy

Mice were deeply anesthetized and perfusion fixed with 4% (w/v) formaldehyde in 0.1 M phosphate buffer (pH 7.4). Tissue pieces from dorsal skin were further postfixed with 2.5% (v/v) glutaraldehyde in phosphate buffer, followed by 1% (w/v) aqueous OsO_4, enbloc stained with 0.5% (w/v) aqueous uranyl acetate and embedded in Epon epoxy resin. Alternatively, skin pieces were processed by means of immersion fixation as described (Lorenz et al., 2007). Primary keratinocytes cultured on collagenI-fibronectin-laminin322 (gift from M. Aumailley) coated Thermanox-coverslips (NUNC) were fixed with 2.5% (v/v) glutaraldehyde in 0.1% (w/v) cacodylate buffer and further processed as described for skin samples. Thin sections (60-100 nm) were analyzed with a Philips CM120 (FEI) or EM902A (Zeiss) microscope, and images were recorded with a MORADA or MegaViewIII digital camera (Olympus SIS). Contrast and brightness were optimized by using gray scale modification and high-pass filtering using Adobe Photoshop software.

Pre-embedding immunogold labeling of primary keratinocytes was performed according to standard protocols. Briefly, cells were fixed with 4% (w/v) phosphate-buffered formaldehyde, rinsed, permeabilized with 0.05% (v/v) Triton-X and labeled with rabbit anti-caveolin-1 (N-20, from Santa Cruz Biotech). Bound antibodies were detected with goat-anti-rabbit secondary antibody coupled to Nanogold (Nanoprobes), followed by silver enhancement of the 1.4 nm-ultrasmall Nanogold particles with HQ silver (Nanoprobes). Finally, samples were shortly post-fixed with OsO_4 and embedded in Epon.

Immunogold labeling of thawed cryosections was performed for skin samples and primary keratinocytes fixed with 4% (w/v) formaldehyde essentially as described previously (Taub et al.,

2007). Formaldehyde-fixed skin samples were additionally stabilized before standard processing for cryosectioning by high-pressure freezing, freeze-substitution and rehydration (van Donselaar et al., 2007), to improve ultrastructure preservation. The antibody against caveolin-1 was from Santa Cruz Biotech (N-20), and the secondary antibodies conjugated to colloidal gold from British Biocell. The relative distribution of caveolin-1 immunogold label in primary keratinocytes was estimated by counting gold particles from randomly selected electron micrographs (primary magnification x19500-31000) that showed more than 7 gold particles per cytoplasmic area (2-9 μm^2). The average depth of caveolae in these samples was 53-75 nm and the length of 2 linked IgG molecules 25 nm. Thus, gold labeling within a distance of <100 nm from the plasma membrane was classified as „peripheral", the residual gold as „intracellular". 15 cell profiles per genotype were quantified.
Quantification of basal caveolae in skin and primary cells was done on randomly chosen electron micrographs from Epon resin sections cut perpendicularly to the BM or culturing plane (skin: >10 cells from three animals per genotype; ILK-K5 keratinocytes: >15 cells from 2 animals per treatment). In case of taxol-treated ILK-K5cells, caveolae were counted only from cells that showed at least 1 caveola per 5µm length of basal plasma membrane (the average length of plasma membrane in x25000 micrographs).

Biofunctionalized micropatterned substrates
The micropatterns were generated on PEG-coated glass coverslips with deep UV lithography (adapted from Azioune et al., 2009). Briefly, glass coverslips were incubated in a 1 mM solution of a linear PEG, CH_3-(O-CH_2-CH_2)$_{43}$-NH-CO-NH-CH_2-CH_2-CH_2-Si(OEt)$_3$, in dry toluene under a nitrogen atmosphere for 20 h at 80 °C. The substrates were removed, rinsed intensively with ethyl acetate, methanol and water, and dried with nitrogen (Blummel et al., 2007). Pegylated glass substrates were then placed onto a chromium synthetic quartz photomask (ML&C, Jena) covered with 1.65 µL of DMSO that provides a spacing of about 5 µm in thickness. The mask-covered substrates were exposed to deep UV light in air using a low-pressure mercury lamp (Heraeus Noblelight GmbH, NIQ 60/35 XL longlife lamp, quartz tube, 60 W) at 5 cm distance for 8 min. The patterned substrates were subsequently incubated with fibronectin (20µg/ml) in 100 mM $NaHCO_3$ (pH 8.5) for 1h at room temperature and washed twice with PBS.

Cre-mediated deletion of β1 integrin
Adenoviral vectors containing the Cre recombinase were produced by transient transfection of AD-293 cells. Viral particles were purified using the AdEasy Virus Purification Kit (Stratagene). Primary keratinocytes were isolated from β1 floxed/floxed mice, and 150 000 cells were plated on fibronectin/collagen coated 30-mm cell culture dishes containing glass coverslips. After 5 d of culture the cells were infected with adenovirus (MOI=113). 4 d later cells were fixed for immunostaining.

Rac membrane association assay
Rac membrane association was analyzed essentially as described previously (del Pozo et al., 2004). Briefly, cells were washed with 10 mM Hepes pH 7.5, 140 mM NaCl and lysed in cold hypotonic buffer (10 mM Hepes pH 7.5, 1.5 mM MgCl2, 5 mM KCl, 1 mM DTT, protease and phosphatase inhibitors). Lysates were incubated for 5 min and homogenized using a Dounce homogenizer. Homogenates were centrifuged at 700 g for 3 minutes to pellet nuclei and intact cells. An aliquot of the supernatant was collected as the total cell extract. The supernatants were then spun at 40,000 g for 30 min to sediment membranes. The cytosol-containing supernatant was removed and the crude membrane pellet gently washed with hypotonic lysis buffer. Total, cytosol, and membrane fractions were then assayed for total protein content and analyzed by Western blotting.

Isolation of detergent resistant membranes (DRMs)
DRMs were prepared essentially as described previously (Lingwood and Simons, 2007). Briefly, cells were lysed on ice in 1% Triton X-100 in TNE-buffer (50 mM Tris-HCl, 150 mM NaCl, 2 mM EDTA, pH 7.4), homogenized using a 23-gauge needle and adjusted to a final density of 40% iodixanol by the addition of OptiPrep Density Gradient Medium (Sigma). Samples were then placed in a centrifuge tube and overlaid with a discontinuous 30%/5% iodixanol density gradient. Samples were centrifuged at 39.000 rpm for 18 h. After centrifugation 1-ml fractions were collected and analyzed by Western blotting.

FRAP
FRAP measurements were performed with an Axiovert 200 (Zeiss) microscope, a CSU10 spinning disc confocal scanhead (Yokogawa) and a Cool-Snap-HQ2 camera (Roper scientific), using a 100x oil objective. Acquisition was controlled by Metamorph Software (Molecular Devices). Images were collected before, directly after and during recovery of bleaching with a rate of 1 frame/5s. Recovery after bleaching was calculated as described previously (Tagawa et al., 2005). Briefly, fluorescent intensity (I) was measured from the whole cell as well as the bleached area before bleaching (=$I_{[0]}$) and during recovery (=$I_{[t]}$). Relative fluorescent intensity (RI) was then calculated according to the following equation $RI=(I_{total[0]}/I_{bleached[0]}) \times (I_{bleached[t]}/I_{total[t]})$. Unspecific bleaching during image acquisition is corrected in this equation. Speed of individual vesicles was measured by manual tracking using the Metamorph software.

siRNA
siRNA duplexes for mDia1, IQGAP1 and scrambled control were from Sigma. Two mDia1 siRNA duplexes (5'-CCCAAUUCUGCUCAUAGAA-3' and 5'-GUUGAUCAAAUGAUUGAUA-3') and two IQGAP1 siRNA duplexes (5'-GUAUGAAGGAGUUGCAGUU-3' and 5'-CUUCGAAAUUGGUCCAACA-3') were used. siRNAs were transfected using Lipofectamine 2000 (Invitrogen) and experiments were carried out 48 h after transfection.

Integrin cell surface expression
Flow cytometry for integrin cell surface expression was performed essentially as previously described (Czuchra et al., 2006). Briefly, 500.000 keratinocytes were washed in 1% BSA/PBS and incubated with FITC-labeled β1 integrin antibodies or IgM isotype controls (both from Pharmingen) in 24 mM Tris-HCl pH7.4, 137 mM NaCl, 2.7 mM KCl for 10 minutes at room temperature followed by 30-40 minutes incubation on ice. Cells were then washed in 1% BSA/PBS, supplemented with propidium iodide and analyzed by flow cytometry.

SUPPLEMENTAL REFERENCES

Azioune, A., Storch, M., Bornens, M., Thery, M., and Piel, M. (2009). Simple and rapid process for single cell micro-patterning. Lab Chip *9*, 1640-1642.

Blummel, J., Perschmann, N., Aydin, D., Drinjakovic, J., Surrey, T., Lopez-Garcia, M., Kessler, H., and Spatz, J. P. (2007). Protein repellent properties of covalently attached PEG coatings on nanostructured SiO(2)-based interfaces. Biomaterials *28*, 4739-4747.

Czuchra, A., Meyer, H., Legate, K. R., Brakebusch, C., and Fässler, R. (2006). Genetic analysis of beta1 integrin "activation motifs" in mice. J Cell Biol *174*, 889-899.

del Pozo, M.A., Alderson, N.B., Kiosses, W.B., Chiang, H., Anderson, R.G.W., and Schwartz, M.A. (2004). Integrins Regulate Rac Targeting by Internalization of Membrane Domains. Science *303*, 839-842.

Lingwood, D., and Simons, K. (2007). Detergent resistance as a tool in membrane research. Nat Prot *2*, 2159-2165.

Lorenz, K., Grashoff, C., Torka, R., Sakai, T., Langbein, L., Bloch, W., Aumailley, M., and Fässler, R. (2007). Integrin-linked kinase is required for epidermal and hair follicle morphogenesis. J Cell Biol *177*, 501-513.
Tagawa, A., Mezzacasa, A., Hayer, A., Longatti, A., Pelkmans, L., and Helenius, A. (2005). Assembly and trafficking of caveolar domains in the cell: caveolae as stable, cargo-triggered, vesicular transporters. J Cell Biol *170*, 769-779.
Taub, N., Teis, D., Ebner, H. L., Hess, M. W., and Huber, L. A. (2007). Late endosomal traffic of the epidermal growth factor receptor ensures spatial and temporal fidelity of mitogen-activated protein kinase signaling. Mol Biol Cell *18*, 4698-4710.
van Donselaar, E., Posthuma, G., Zeuschner, D., Humbel, B. M., and Slot, J. W. (2007). Immunogold labeling of cryosections from high-pressure frozen cells. Traffic *8*, 471-485.